ELSEVIER

Journal of Materials Processing Technology 113 (2001) 373–377

Journal of Materials Processing Technology

www.elsevier.com/locate/jmatprotec

A finite element model for the orthogonal cutting of fiber-reinforced composite materials

Mofid Mahdi, Liangchi Zhang*

Department of Mechanical and Mechatronic Engineering, The University of Sydney, Sydney, NSW 2006, Australia

Abstract

The tendency towards increased automation of composite cutting operations stimulates the investigation of cutting force evaluation. Different from the conventional method of modeling, which often assumes a continuous chip formation with a predefined separation layer, this study considered the chip breaking and developed a 2D cutting force model with the aid of the finite element method. The variation of the cutting force was investigated carefully against both the cutting conditions and the anisotropy of the material with the following development: (a) a constitutive model of a homogeneous anisotropic elastic material under plane deformation; (b) a failure model of the work-material based on the Tsai–Hill criterion; and (c) a contact model of the mechanisms of the cutting process. A comparison with experimental measurements showed that the constitutive model leads to a reasonable prediction.

Keywords: Finite element method; Orthogonal cutting; Anisotropic composite

1. Introduction

Generally, a composite material is made from a matrix and a much stronger reinforcing material. When compared with conventional single-phase materials, composites have a smaller weight to strength ratio and favorable directional properties, which can be tailored to meet the specific requirements of a design. However, these special properties also make the cutting of composites very difficult, although various cutting methods such as laser, water jet, electron beam and conventional machining techniques have been developed. For example, Aronson [1] considered different methods of the machining of composite materials and summarized the major differences in relation to other materials. Wern et al. [2] conducted a photo-elastic study to examine the stress fields in the cutting process of fiber-reinforced plastics (FRPs) considering the forces and cutting mechanisms in relation to fiber angle. Santhanakrishnan et al. [3] highlighted the machinability of FRP composites, surface production, tool wear and some associated mechanisms. Inoue [4] investigated the fracture mode of glass yarn of a special unidirectional glass FRP specimen cut orthogonally under dry conditions in order to explore the machining characteristics. The effects of the direction of the yarn and the radius of the cutting edge on the cut surface, the failure of the yarn and the cutting force were considered. Spur and Wunsch [5] conducted a study of the surface finish, cutting forces, temperature and the extent of tool wear when turning various fiber composite materials. Hashish [6] detailed quantitative and qualitative results of abrasive-water jet (AWJ) machining of metal matrix composites, laminated thermoset composites and ceramic composites under different conditions. Hamatani and Ramulu [7] conducted an experimental investigation on the machinability of particulate reinforced ceramic composites by an abrasive water jet and showed the satisfaction of the method in terms of cut quality and machined surface characteristics. Hung et al. [8] presented research results on the ultra-precision machining of a metal matrix composite (MMC) composed of aluminum matrix and either SiC or Al_2O_3 particles. They evaluated the ductile-regime machining of both SiC and aluminum to improve the surface integrity of the composite and proposed a model to calculate the critical depth of cut. Wang and Zhang [9,10] investigated the cutting of carbon fiber-reinforced composite and found that the machinability and surface integrity are mainly controlled by the fiber orientations and curing conditions.

The direct experimental approach to study machining processes as outlined above is expensive and time consuming. Alternative methods are numerical simulation and analytical models. Amongst the numerical procedures, the finite element method (FEM) has been the most effective.

* Corresponding author. Fax: +61-29351-3760.
E-mail address: zhang@mech.eng.usyd.edu.au (L. Zhang).

0924-0136/01/$ – see front matter
PII: S0924-0136(01)00675-6

Koca and Buchholz [11] did an analytical stress analysis for a 3D fiber/matrix composite cylinder of finite length subjected to a stationary and homogeneous change of temperature with respect to the stress free state. Puw et al. [12,13] presented the cutting mechanisms and the failure of composite material in relation to the fiber direction and constructed a correlation between cutting force and the produced chip length using beam theory, linear elastic fracture mechanics and composite mechanics. They also presented an anisotropic mechanistic model for the force prediction in the milling of continuous fiber-reinforced composite materials. Bhatnagar et al. [14] made an observation on the orthogonal machining of unidirectional carbon fiber-reinforced plastic (UD-CFRP) laminates, and based on that proposed a model for predicting the cutting forces. Wern and Ramulu [15] proposed some semi-empirical models and investigated the behavior of two idealized FRP composites to examine the effects of ductile and brittle reinforcements, fiber orientation, cutting tool geometry, depth of cut and cutting speed on the machining process. Chandrasekharan et al. [16] developed and calibrated models to predict the thrust and torque forces at the different regions of cutting on a drill. Arola and Ramulu [17] analyzed the orthogonal cutting of unidirectional fiber-reinforced polymer composites using the FEM. They used a dual fracture process to simulate chip formation incorporating both the maximum stress and Tsai–Hill failure criteria. They also highlighted the influence of fiber orientation and tool geometry on the fracture stress and discussed their effects on the material removal process in the orthogonal trimming of reinforced polymers. However, the FEM mesh was based on experimental investigations. Recently, the present authors [18] considered the effects of the threshold of chip separation criteria and the local rake angle on the orthogonal cutting force behavior and the residual stresses.

The above review indicates that further improvement of the basic finite element modeling is essential to deeply understand the cutting mechanics of composites. In the present paper, a 2D cutting model is presented to predict the cutting force behavior of composites in relation to fiber angle. The chip separation criterion and the material properties are particularly addressed.

2. Finite element model of cutting

The cutting is approximated as a quasi-static plane problem. To model the contact, the cutting tool is assumed to be rigid while the workpiece is defined by the elastic properties of each of the constituents, i.e., fibers and matrix. The cutting tool is considered as a target and the workpiece as a contactor [19]. For simplicity, friction is ignored.

2.1. Control volume and boundary conditions

A predefined ramp scaling function (time function) is applied to simulate the movement of the cutting tool. The workpiece is taken as stationary such that the nodes at the workpiece base are fixed. The cutting tool has a predefined movement (displacement boundary conditions) in the negative x-direction (with velocity v) as illustrated in Fig. 1. The total number of nodes is 1525. The nominal cutting depth is 2 mm. The depth and length of the control volume are 5 and 10 times the cutting depth, respectively. To model the cutting tool geometry, six nodes were used. The total number of elements is 360 nine-node elements. To predict the effect of mesh size on the cutting force, a coarser finite element mesh with 180 elements was also used in Fig. 1b.

2.2. Material properties

The structure of unidirectional composite material has periodic microstructure properties that vary in a repetitive pattern throughout the body. For cutting force prediction, the properties of the fiber and matrix are used to obtain an equivalent homogeneous anisotropic material (EHAM), thereby the resulting macro-stiffness of EHAM is that of the combined fiber and matrix structure. This homogenization can be used for determining the equivalent global properties of the work-material and the basic idea is to

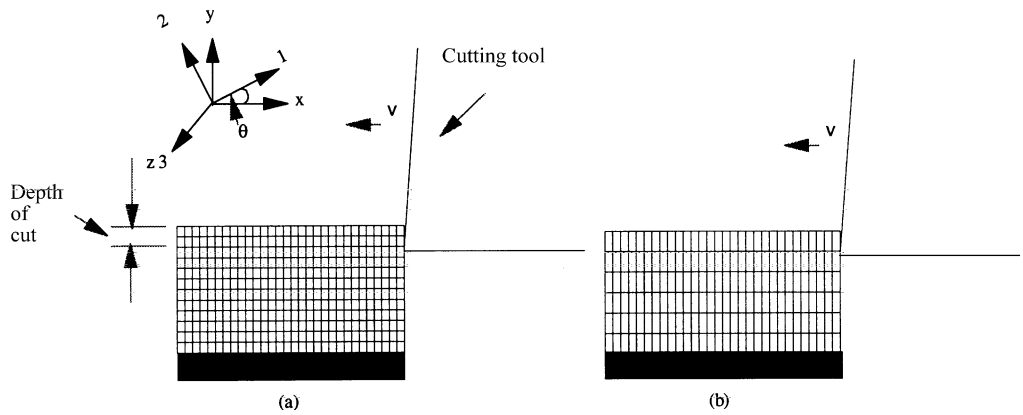

Fig. 1. FEM mesh and cutting geometry: (a) fine mesh; (b) coarse mesh.

make use of individual fiber and matrix properties incorporating their volume ratio and fiber angle. Both the fiber and matrix materials are assumed to be isotropic. Young's moduli of the fiber and matrix are $E_f = 237\,\text{GPa}$ and $E_m = 2.96\,\text{GPa}$, respectively. The Poisson ratios are both 0.35. With the aid of the theory presented by Chamis [20], the properties of EHAM are calculated as $E_2 = 120\,\text{GPa}$, $E_1 = E_3 = 9.81\,\text{GPa}$, $G = 3.63\,\text{GPa}$ and $v_{12} = v_{13} = v_{23} = 0.35$, where 2 refers to the direction of the fiber and 1 and 3 refer to the other transverse directions. Moreover, $v_{12} = E_{11}/E_{22}v_{21}$, $v_{13} = E_{11}/E_{33}v_{31}$ and $v_{23} = E_{22}/E_{33}v_{32}$ should hold. Fig. 1 shows the conventions of material axis and geometric axis (i.e. 1, 2, 3 and x, y, z). By using the homogenization procedure and the FEM, the global constitutive behavior of the corresponding orthotropic material can be expressed by the symmetric stiffness matrix, D, as

$$D = \begin{bmatrix} \dfrac{E_{11}}{1-v_{12}v_{21}} & \dfrac{v_{12}E_{22}}{1-v_{12}v_{21}} & 0 & \dfrac{v_{13}E_{33}}{1-v_{13}v_{31}} \\ & \dfrac{E_{22}}{1-v_{12}v_{21}} & 0 & \dfrac{v_{23}E_{33}}{1-v_{23}v_{32}} \\ & & \dfrac{1}{G} & 0 \\ \text{Sym.} & & & \dfrac{E_{33}}{1-v_{13}v_{32}} \end{bmatrix} \tag{1}$$

If the material axis and the geometrical axis do not coincide, the stiffness matrix D needs to be replaced by Q [21]:

$$Q = [T]_\sigma^{-1} D [T]_\varepsilon \tag{2}$$

where $[T]_\sigma$ and $[T]_\varepsilon$ are the transformation matrixes for stresses and strains, respectively, defined as

$$[T]_\sigma = \begin{bmatrix} m^2 & n^2 & 2mn & 0 \\ n^2 & m^2 & -2mn & 0 \\ -mn & mn & m^2-n^2 & 0 \\ 0 & 0 & 0 & 1 \end{bmatrix}$$

$$[T]_\varepsilon = \begin{bmatrix} m^2 & n^2 & mn & 0 \\ n^2 & m^2 & -mn & 0 \\ -2mn & 2mn & m^2-n^2 & 0 \\ 0 & 0 & 0 & 1 \end{bmatrix} \tag{3}$$

where $m = \cos(\theta)$, $n = \sin(\theta)$ and θ is the fiber angle difference.

The above formulation can be realized using the user-supplied option of ADINA. To verify the reliability, the directional elastic stiffness (DES) obtained by relevant models were compared with the corresponding analytical solutions as demonstrated in Fig. 2. It shows that they are almost identical and therefore the developed material model is accurate to simulate the work-material behavior under the given cutting conditions. In this non-linear analysis, the updating of the stiffness matrix was based on a full-Newton scheme and line search with a set limit of 15 iterations per increment. The SPARSE SOLVER, which ensures the positive definiteness of the global stiffness matrix, was used for a greater efficiency in the solution of the equilibrium equations. A displacement-based convergence tolerance was used with the automatic reduction of the time-stepping increment whenever necessary.

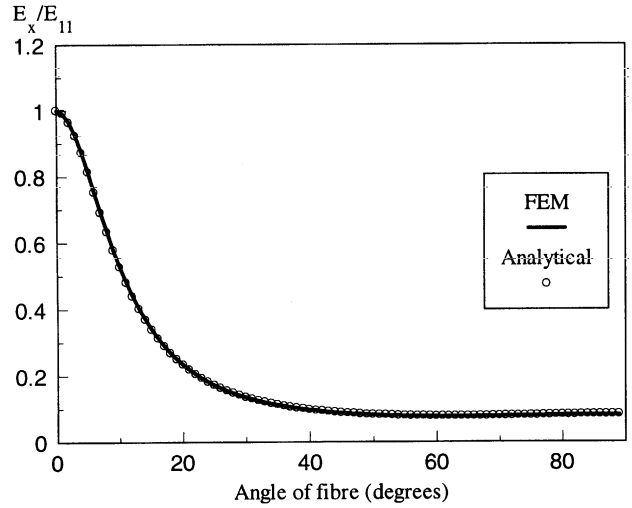

Fig. 2. Directional stiffness of an anisotropic material: analytical vs. FEM solution.

2.3. Cutting criteria

It is of central importance to be able to predict the strength of composite under the loading conditions of an orthogonal cutting. To achieve this, the use of a proper material separation criterion plays a key role as it provides information about the failure under combined stresses. There are a number of separation criteria based on the maximum stress, strain and work theories [22]. In this context, the Tsai–Hill (or maximum work) criterion is applied to simulate the formation of chips and thereby the material separation during cutting. For an orthotropic lamina under plane-stress conditions, the failure or separation will occur when

$$\frac{\sigma_1^2}{X_1^2} - \frac{\sigma_1\sigma_2}{X_1^2} + \frac{\sigma_2^2}{X_2^2} + \frac{\sigma_{12}^2}{S^2} \geq 1 \tag{4}$$

where X_1 and X_2 are the tensile (or compressive) failure strength in the 1 and 2 directions and S the shear failure strength. As the global stresses (σ_{xx}, σ_{yy}, σ_{xy}) are calculated based on global coordinates x, y and z, they need to be transformed back to material axes 1 and 2, i.e. σ_{11}, σ_{22} and σ_{12} by

$$\begin{bmatrix} \sigma_{11} \\ \sigma_{22} \\ \sigma_{12} \\ \sigma_{33} \end{bmatrix} = [T]_\sigma \begin{bmatrix} \sigma_{xx} \\ \sigma_{yy} \\ \sigma_{xy} \\ \sigma_{zz} \end{bmatrix} \tag{5}$$

During cutting simulation, Eqs. (4) and (5) are evaluated to predict the formation of chips. The failure strengths of EHAM are $X_1 = 60.4\,\text{MPa}$, $X_2 = 2.6287\,\text{GPa}$ and $S = X_1/\sqrt{2}$.

2.4. Contact modeling

The contact analysis is based on segmental-method to achieve a more powerful convergence, with a convergence factor of 0.05. The cutting tool surface and a node in the workpiece body make up a target–contactor pair such that the contactor may become a new node as the cutting tool advances. The cutting forces are then calculated as the summation of the contact forces exerted on individual contact points.

3. Results and discussion

To study the effect of the finite element mesh size shown in Fig. 3, the cutting force of an isotropic work-material is computed for both plane-stress and plane-strain conditions using the maximum shear failure criterion for chip formation. It is found that the control volume with the finer mesh will not only smooth the variation of cutting force with the shear stress threshold but also lower its magnitude. On the other hand, the control volume with the finer mesh results in identical cutting forces for both plane-stress and plane-strain conditions. This indicates that the finite element mesh size used may be adequate for this analysis as far as the cutting force prediction is concerned.

The effect of mesh size on the solution accuracy of cutting force is also analyzed for an anisotropic material with the Tsai–Hill criteria for chip production as shown in Fig. 4. The results show a similar trend to that of the isotropic work-material in terms of their smoothness and magnitudes. The cutting forces of plane-strain and plane-stress conditions reach their maximum when the fiber angle is around 100°. Moreover, the forces associated with the plane-stress condition of cutting are greater. This is related to the fact that the plane-stress state of cutting results in a lower stress threshold as one stress component is zero. Thus a higher stress level is required to satisfy the failure criterion. In turn a larger cutting force is needed to form chips.

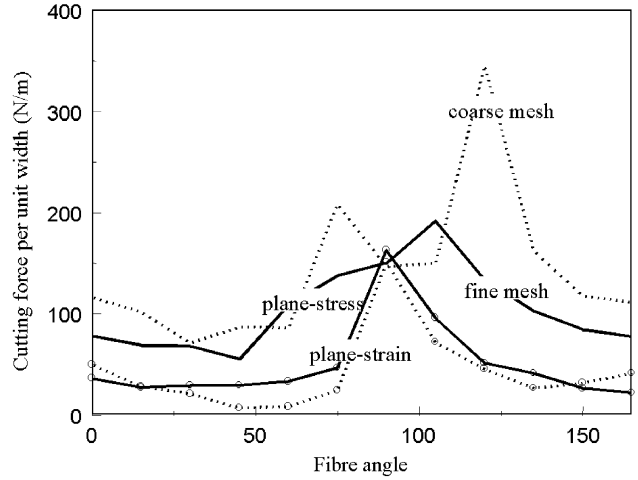

Fig. 4. The mesh refining effect of an anisotropic material cutting force.

Fig. 5 demonstrates the comparison of the cutting forces with experimental results obtained by Wang and Zhang [9]. The model predictions are in good agreement with experimental measurement in general. Clearly, the rake angle of the cutting tool, varying from 0° to 20°, does not have a remarkable effect, as the comparison shows. The difference between the experimental and theoretical results may be due to the homogenization procedure of the material properties, because the micro-effect of fibers may be considerable.

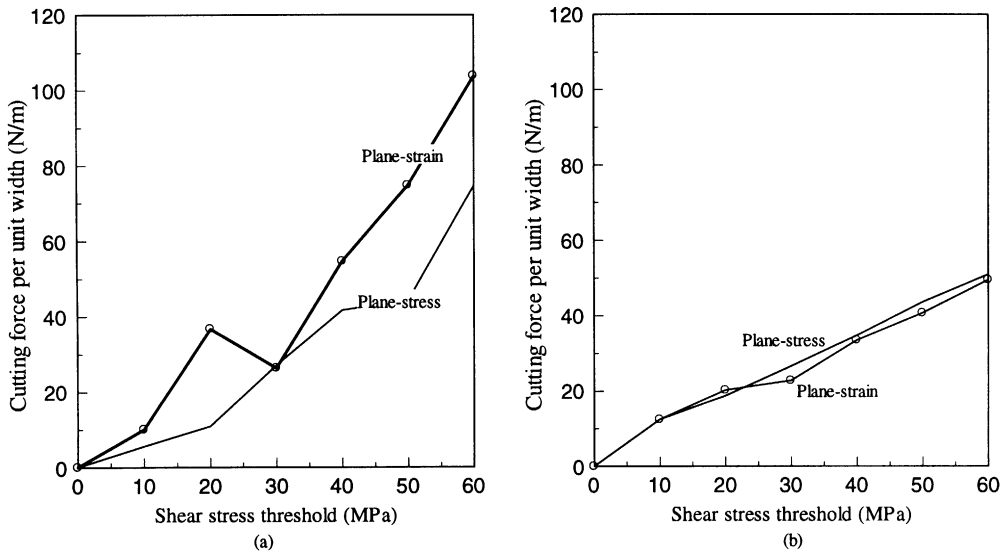

Fig. 3. Cutting force vs. shear stress threshold of an isotropic material mesh refining effect: (a) coarse mesh; (b) fine mesh.

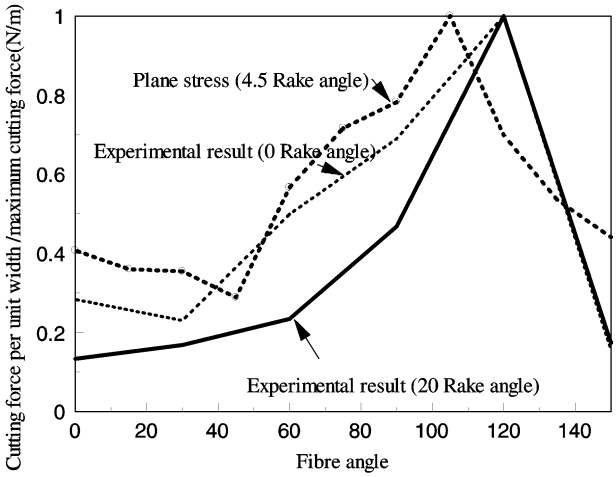

Fig. 5. Cutting force vs. fiber angle of an anisotropic material.

4. Conclusion

An user-defined constitutive material model for an anisotropic work-material has been developed to investigate the variation of the cutting forces with the fiber angle of a composite material. When using the Tsai–Hill criterion for the chip separation and the segmental contact treatment, the model leads to a reasonable prediction compared with corresponding experimental measurements.

Acknowledgements

The financial support from ARC to the present study is appreciated. The ADINA code was used for all the calculations.

References

[1] B.A. Robert, Manuf. Eng. 122 (1) (1999) 52.
[2] C.W. Wern, M. Ramulu, A. Shukla, Exp. Mech. 36 (1) (1996) 33.
[3] G. Santhanakrishnan, R. Krishnamurthy, N.G. Nair, Machine Tool Design and Research Conference, Delhi, India, 1986, p. 299.
[4] H. Inoue, Zairyo/J. Soc. Mater. Sci. 36 (402) (1987) 242.
[5] G. Spur, U.E. Wunsch, German Plastics 76 (3) (1986) 8.
[6] M. Hashish, Manuf. Rev. 2 (2) (1989) 142.
[7] G. Hamatani, M. Ramulu, Mach. Composites 35 (1988) 49.
[8] N.P. Hung, T.C. Tan, Z.W. Zhong, G.W. Yeow, Mach. Sci. Technol. 3 (2) (1999) 255.
[9] X.M. Wang, L.C. Zhang, in: Abrasive Technology: Current Development and Applications, Vol. I, World Scientific, Singapore, 1999, p. 429.
[10] X.M. Wang, L.C. Zhang, in: Progress of Machining Technology, Aviation Industry Press, Beijing, 2000, p. 13.
[11] O. Koca, F.G. Buchholz, Comput. Mater. Sci. 3 (2) (1994) 135.
[12] H.Y. Puw, H. Hocheng, H.C. Kuo, Manufacturing Science and Engineering Proceedings, 1995, p. 259.
[13] H.Y. Puw, H. Hocheng, Proceedings of the Third Biennial Joint Conference on Engineering Systems Design and Analysis, 1996, p. 11.
[14] N.R. Bhatnagar, N.K. Naik, R. Komanduri, Int. J. Mach. Tools Manuf. 35 (5) (1995) 701.
[15] C.W. Wern, M. Ramulu, Proceedings of the 1995 Machining of Advanced Materials, 1995, p. 1.
[16] V. Chandrasekharan, S.G. Kapoor, R.E. DeVor, Proceedings of the 1993 Machining of Advanced Composites, 1993, p. 33.
[17] D. Arola, M. Ramulu, Int. J. Mech. Sci. 39 (5) (1997) 597.
[18] M. Mahdi, L.C. Zhang, in: Abrasive Technology: Current Development and Applications, Vol. I, World Scientific, Singapore, 1999, p. 337.
[19] ADINA, Theory and Modeling Guide — ADINA Report ARD97-9, 1997.
[20] C.C. Chamis, NASA Tech. Memo 83320, 1983.
[21] Chawla, Krishan Kumar, Composite Materials: Science and Engineering, Springer, Berlin, 1987.
[22] L.C. Zhang, J. Mater. Proc. Technol. 89–90 (1999) 273–278.